

## Errors in high-latitude SSTs and other geophysical products linked to NOAA-14 AVHRR channel 4 problems

Guillermo P. Podesta

University of Miami, Rosenstiel School of Marine and Atmospheric Science, Miami, Florida, USA

Manuel Arbelo

Departamento de Física, Universidad de La Laguna, La Laguna, Islas Canarias, Spain

Robert Evans, Katherine Kilpatrick, Vicki Halliwell and James Brown

University of Miami, Rosenstiel School of Marine and Atmospheric Science, Miami, Florida, USA

**Abstract.** Errors in brightness temperatures for channel 4 in the Advanced Very High Resolution Radiometer (AVHRR) onboard the NOAA-14 spacecraft are examined. The errors involve a low frequency of occurrence for some values, and a corresponding enhancement of frequency for others. Errors appear to be related to the conversion of analog to digital values. Unfortunately, it is not possible to identify and separate erroneous values. The most apparent errors in geophysical products derived from AVHRR's channel 4 occur at low brightness temperatures, therefore sea surface temperatures in high latitudes (below about 6°C) and cloud-related products must be used with caution, as they may have systematic errors as large as 0.5°C.

### 1. Introduction

Space-based multichannel infrared (IR) radiometers operating in cloud-free conditions provide the most reliable global sea surface temperature (SST) data sets [Barton, 1995]. Consistently reprocessed SST series derived from operational instruments such as the AVHRR (Advanced Very High Resolution Radiometer) onboard NOAA polar-orbiting satellites have reached a length (about two decades) that begins to allow a characterization of the ocean's climate. Of course, to use satellite SST estimates in climate studies, the values must be as accurate and bias-free as possible.

It is difficult to validate synoptic, global satellite-derived SST fields with in situ measurements that frequently have a sparse geographic/temporal distribution. An alternative is to compare SST fields from different sensors. For example, Fig. 1a shows differences between nighttime global SST fields from the MODIS (MODerate resolution Imaging Spectroradiometer) instrument onboard the Terra spacecraft and the NOAA-16 AVHRR, averaged over the period 31 October 2000 to 8 September 2001.

Fig. 1b shows differences between SST fields for the same period from AVHRRs onboard NOAA-14 and NOAA-16. A striking feature of Fig. 1b is a large geographic area at high latitudes with consistently high differences ( $< -0.5^{\circ}\text{C}$ ) in SST estimates: NOAA-14 SST is significantly colder than NOAA-16 below SSTs of about 4°C (the contour overlaid on Fig. 1b). Because

this difference is not apparent in the comparison of NOAA-16 and MODIS SSTs (Fig. 1a), concerns are raised about the accuracy of NOAA-14 SSTs. The goal of this paper is to explore errors in NOAA-14 AVHRR data and to alert users of SST and other geophysical products derived from this sensor about potential problems for conditions associated with low channel 4 brightness temperature values.

### 2. The Data: SST Fields and Satellite-in situ Matchups

NOAA-14 and -16 SST values shown in Fig. 1 have been computed using the Pathfinder SST algorithm [Kilpatrick et al., 2001] which has the same form for both NOAA-14 and NOAA-16 data, except for differences in the algorithm coefficients. The MODIS instrument onboard NASA's Terra spacecraft views the Earth in a range of wavelengths, including mid-wave and thermal infrared channels similar to those of the AVHRR. The MODIS SST 11-12  $\mu\text{m}$  algorithm is described in Brown and Minnett [1999] and is based on the Pathfinder algorithm formulation.

To explore potential problems with inputs to the NOAA-14 SSTs, we used a database of "matchups", or co-located, co-temporal in situ SST measurements by moored and drifting buoys, and AVHRR observations. The matchups encompass the period from 25 January 1995 (the beginning of NOAA-14's operational lifetime) to 31 December 1999. Further information on the AVHRR Pathfinder matchup database is available at [<http://www.rsmas.miami.edu/groups/rsl/pathfinder/>].

### 3. Problems with AVHRR Brightness Temperatures and SST Values

Inputs to the AVHRR Pathfinder SST algorithm include brightness temperatures from AVHRR channels 4 and 5 (hereafter referred to as T4 and T5) and a first-guess SST value. The first-guess SSTs used to compute Pathfinder SSTs are identical for NOAA-14 and NOAA-16: the NCEP optimally interpolated SSTs [Reynolds and Smith, 1994], thus this quantity cannot introduce the observed differences between NOAA-14 and -16 SST fields. Therefore, attention is focused on T4 and T5 values.

Fig. 2 shows a time series of T4 values in the NOAA-14 matchup database. A gap with a lower density of T4 values is clearly apparent. The location of the gap changes in time. In early 1995, the gap is located at  $1.3^{\circ}\text{C} < \text{T4} < 1.9^{\circ}\text{C}$ . In 1999, the gap appears more populated (because, overall, there are more matchups towards the end of the series), but its boundaries are  $2.4^{\circ}\text{C} < \text{T4} < 3.0^{\circ}\text{C}$ , i.e., more than a degree higher than at the beginning. A similar graph for T5 (not shown) did not reveal such an apparent gap.

The T4 gap is associated not only with SST values missing or being less frequent, but also with errors in SST estimates. Many T4 values in the vicinity of the gap appear to be erroneous and, consequently, introduce errors in SST estimates. Fig. 3 shows SST residuals (in situ minus satellite SSTs) as a function of in situ SST. Two sets of points are plotted. Red circles correspond to matchups below the gap (i.e.,  $\text{T4} \leq 1.5^{\circ}\text{C}$ , the approximate lower boundary of the identified gap for all years). Blue crosses correspond to matchups with  $3.0^{\circ}\text{C} \leq \text{T4} \leq 5.0^{\circ}\text{C}$ ; these points represent conditions immediately above the gap. Matchups below the gap tend to produce positive (median:  $0.43^{\circ}\text{C}$ ) SST residuals, i.e. under-prediction of satellite-derived values. In contrast, matchups just above the gap tend to produce negative (median:  $-0.17^{\circ}\text{C}$ ) residuals, i.e. overprediction of satellite SSTs. Beyond the vicinity of the gap, values do not show systematic errors: for  $\text{SST} \geq 6^{\circ}\text{C}$ , the median of residuals hovers around zero. A similar return to near-zero errors cannot be detected below the vicinity of the gap, as available in situ observations are very sparse.

### 4. What Can Cause the Problems in NOAA-14's T4 Values?

Our motivation for this manuscript is to alert users of NOAA-14 AVHRR data about potential problems in geophysical products for conditions associated with low T4 values. A full characterization of the problem is beyond the scope of this paper, but we can submit preliminary hypotheses about its causes.

The missing and erroneous T4 values for the AVHRR onboard NOAA-14 may be related to problems with the instrument's analog-to-digital converter (ADC). The ADC converts continuous voltages from the

radiometer into discrete values from 0 to 1023 (corresponding to a 10-bit digitization scheme) by successive approximation. A voltage fed into the ADC is compared to an initial threshold (defined by sensor electronics). If the input is greater than this threshold, the highest order bit is set on, otherwise the bit is off. Voltages above and below the initial threshold are then compared to a second layer of thresholds which define the status of the second highest order bit, and so on until all bits are resolved.

If the thresholds in the ADC do not coincide with their nominal values (e.g., as a result of drift in the electronics), then some of the output digital values can be wrong. To illustrate this, we simulate the analog-to-digital conversion. First, we generate a uniform distribution of 16,000 continuous (i.e., "analog") values from 0 to 16. Then, we simulate a 4-bit digitization (i.e., output digital values range from 0 to 15). The thresholds in the digitization are defined such that the distribution of analog values gets successively divided into halves. For instance, the first threshold voltage is defined to be 7.877 (the value that separates the upper and lower halves of the simulated input values). Because of the way we have defined the successive thresholds, all resulting digital values from 0 to 15 have the same frequency of occurrence (1000). The second step is to simulate a small upward shift in the threshold for the highest-order bit (from 7.877 to 8.822, or about 12%). Such a shift may occur by problems in ADC electronics. As a consequence, the frequency of digital values equal to 7 increases from 1000 to 1936 (Fig. 4). Conversely, the bin with digital values of 8 is almost empty (it only has 64 records).

This example illustrates how a problem with the AVHRR's ADC may result in a gap (or underpopulation) for certain digital values. The "missing" values from bin 8, however, are included in adjacent bin 7, enhancing artificially the frequency of records in this bin. In other words, many of the values in bin 7 are wrong (they should have been allocated to bin 8). If the simulated output represented AVHRR channel 4 digital counts and the erroneous values from bin 7 were used in an SST algorithm, the resulting SSTs would be underpredicted. Unfortunately, incorrect values within bin 7 cannot be recognized and isolated from those that are correct. A prudent course of action, therefore, is to assume that quantities derived from values in this bin potentially may be wrong.

### 5. Observed AVHRR Digital Values

To confirm the presence of potential problems in the NOAA-14 AVHRR ADC, we extracted digital counts for channels 4 and 5 for ocean areas south of  $40^{\circ}\text{S}$  during 31 October to 2 November 2000. For comparison, we also extracted NOAA-16 AVHRR channel 4 data for the same dates and region. Fig. 5 shows the frequency distribution of all these digital

values (the distributions are shifted because calibration differs between channels and sensors).

There is a clear decrease in the frequency of channel 4 values around count 511. This value corresponds to the middle of the overall digital range, and thus is associated with the ADC threshold for the highest-order bit. However, we have detected similar problems around digital values associated with transitions ( $2n$ ) in lower-order bits. For instance, there are deficits/increases in the number of NOAA-14 channel 4 pixels with digital values around 255-256 (histograms not shown). As there is a single digitizer for all AVHRR channels, we would expect similar problems in channel 5 as well. Nevertheless, there is only a slight decrease in channel 5 frequency of occurrence around digital count 511. Finally, the marked decrease in number of NOAA-14 pixels around count 511 is not apparent for NOAA-16 channel 4, suggesting that the ADC problem does not occur in every AVHRR. Further, the NOAA-16 line is much smoother, suggesting that the ADC in this instrument is less noisy.

The final step is to verify that the NOAA-14 channel 4 digital counts around 511 coincide approximately with the T4 brightness temperatures where the problems occur (Fig. 2). Using published NOAA sensor calibration, lookup tables were derived for NOAA-14 channel 4 for early November of 1995, 1997, and 1999. For the three years, channel 4 brightness temperatures corresponding to digital value 511 (averaged over various scenes) were about 1.7°C, 2.2°C, and 2.5°C (indicated with large circles in Fig. 2). The shift in the location of the gap, therefore, is due to temporal changes in calibration of channel 4 (the conversion of digital counts into brightness temperatures) resulting, e.g., from changes in the sensor operating temperature.

The NOAA-14 AVHRR has the same technology as those on NOAA-9 and NOAA-11 (the other instruments in the AVHRR Oceans Pathfinder SST data base). There are concerns that ADC issues may be present in these instruments as well. As a preliminary assessment, we extracted digital counts south of about 40°S for three days of NOAA-9 (1-3 November 1985) and four days of NOAA-11 (12-15 November 1988). We detected deficits and enhancements of the numbers of pixels near count values 511 and 768 (associated with errors in first- and second-order bits, respectively). Nevertheless, the variations were not nearly as pronounced as for NOAA-14. Further diagnostics (encompassing the entire lifetime of all sensors) should be undertaken in the future.

## 6. Conclusions

We report problems in NOAA-14 AVHRR values that are most apparent for channel 4 at low brightness temperatures. These problems apparently are associated with the analog-to-digital conversion of radiances sensed by the AVHRR.

Examples of affected AVHRR-derived geophysical products include SST fields at high latitudes (see Fig. 1), or estimated cloud top temperatures. The AVHRR uses a digitizing scheme where high counts correspond to low brightness temperatures. Thus, low SSTs at high latitudes are predominately affected because the high-order bit is set to on for these conditions, whereas temperate and tropical SSTs are potentially affected by less apparent problems in the low order bits. SST fields apparently are affected between 2 and 6°C, and values may be systematically over- or under-predicted by as much as 0.5°C. Impacts may extend not only to NOAA-14 SST fields, but also to products that rely totally or partially on these data, such as the SST analyses produced by *Reynolds et al.* [2002] or climatologies in *Casey and Cornillon* [1999] and *Sumner et al.* [2003]. Because it is not possible to identify and exclude erroneous input values, all SSTs in the range mentioned need to be considered as potentially biased. The geographic location of the affected SSTs will change in space in response to seasonal variability and the long-term trend due to changes in counts-to-radiance conversion (Fig. 2).

Other examples of affected AVHRR-derived geophysical products include the surface temperature of sea ice in Antarctica (Veihelmann et al., 2001), clear-sky surface-temperature retrieval algorithms developed with data specific for the Arctic and the Antarctic regions, over ocean and land [*Key et al.*, 1997], or methods to discriminate polar stratospheric clouds from other cloud types in AVHRR imagery based on the brightness temperature difference between channels 4 and 5 [*Hervig et al.*, 2001]. Likewise algorithms to eliminate contaminated pixels by clouds using NOAA-14/AVHRR channel 4 brightness temperatures may also need to be revised [*Kilpatrick et al.*, 2001; *Simpson et al.*, 2001; *Chen et al.*, 2002].

**Acknowledgments.** This study was supported by NASA grants “EOS MODIS Oceans Processing Framework and Matchup Database”, and “Continued Processing and Extension of the Pathfinder Oceans SST Global Dataset”. NOAA provided access to Level 0 AVHRR data via DOMSAT. In situ SSTs for the Pathfinder matchup database were provided by NOAA’s PMEL, AOML and NDBC, Canada’s MEDS, the Japanese Meteorological Agency, and the UK Met Office.

## References

- Brown, O, and P. Minnett. MODIS Infrared Sea Surface Temperature Algorithm Theoretical Basis Document v2.0. atbd-25, April 1999. [http://modis.gsfc.nasa.gov/data/atbd/ocean\\_atbd.html](http://modis.gsfc.nasa.gov/data/atbd/ocean_atbd.html)
- Casey, K. S. and P. Cornillon, A comparison of satellite and in situ-based sea surface temperature climatologies, *Journal of Climate*, 12, 1848-1863, 1999.

- Chen, P. Y., R. Srinivasan, G. Fedosejevs, B. Narasimhan, An automated cloud detection method for daily NOAA-14 AVHRR data for Texas, USA, *International Journal of Remote Sensing*, 23, 2939-2950, 2002.
- Hervig, M. E., K. L. Pagan, P. G. Foschi, Analysis of polar stratospheric cloud measurements from AVHRR. *J. Geophys. Res.*, 106, 10363-10374, 2001.
- Key, J., J. Collins, C. Fowler, and R.S. Stone, High-latitude surface temperature estimates from thermal satellite data, *Remote Sensing of the Environment*, 61, 302-309, 1997.
- Kilpatrick K. A., G. P. Podestá, and R. Evans, Overview of the NOAA/NASA advanced very high resolution radiometer Pathfinder algorithm for sea surface temperature and associated matchup database, *Journal of Geophysical Research*, 106, 9179-9197, 2001.
- Reynolds, R. W., and T. M. Smith, Improved global sea surface temperature analyses using optimum interpolation, *Journal of Climate*, 6, 768-774, 1994.
- Reynolds, R. W., N. A. Rayner, T. M. Smith, D. C. Stokes and W. Wang, An improved in situ and satellite SST analysis for climate, *Journal of Climate*, 15, 1609-1625, 2002.
- Simpson J. J., T. J. McIntire, J. R. Stitt and G. L. Hufford, Improved cloud detection in AVHRR daytime and night-time scenes over the ocean, *International Journal of Remote Sensing*, 22, 2585-2615, 2001.
- Sumner, M. D., K. J. Michael, C. J. A. Bradshaw and M. A. Hindell, Remote sensing of Southern Ocean sea surface temperature: implications for marine biophysical models, *Remote Sensing of the Environment*, 84, 161-173, 2003.
- Veihelmann, B., F. S. Olesen, C. Kottmeier, Sea ice surface temperature in the Weddell Sea (Antarctica), from drifting buoy and AVHRR data. *Cold Reg. Sci. Tech.* 33, 19-27, 2001.
- (Received Xxxxxx XX, 2003; revised Xxxxxx XX, 2003; accepted Xxxxxxxxx XX, 2003.)
- G. Podestá, R. Evans, K. Kilpatrick, V. Halliwell and J. Brown, Rosenstiel School of Marine and Atmospheric Science, University of Miami, 4600 Rickenbacker Causeway, Miami FL 33149, USA (email: gpodesta, revans, kkilpatrick, vhalliwell or jbrown@rsmas.miami.edu).
- Manuel Arbelo, Departamento de Física, Universidad de La Laguna, 38200 La Laguna, Islas Canarias, Spain (e-mail: marbelo@ull.es).

**Figure 1.** Differences between nighttime global SST estimates provided by various instruments. (a) MODIS minus NOAA-16 AVHRR, (b) NOAA-14 minus NOAA-16 AVHRR. In both cases, the figures represent an average of daily differences for the period 31 October 2000 to 8 September 2001. The 4°C contour overlaid on Fig. 1b corresponds to MODIS-Terra SST averaged over the period mentioned above.

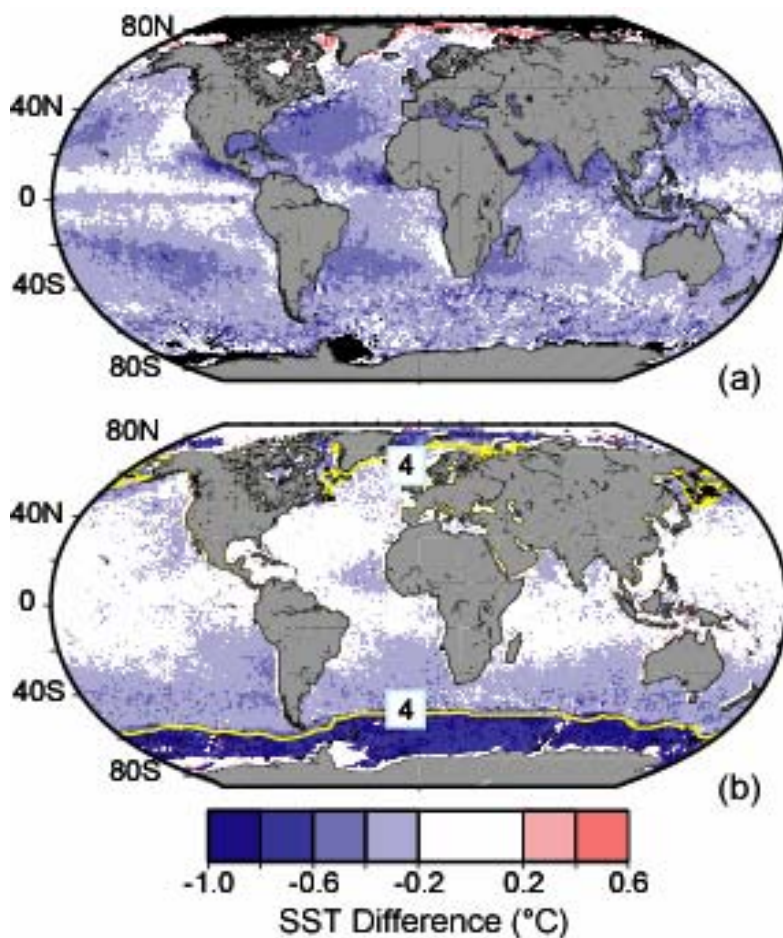


**Figure 2.** Time series of channel 4 brightness temperatures for the AVHRR onboard NOAA-14, from the Pathfinder matchup database. The large circles in the third quarters of 1995 and 1997 indicate the brightness temperatures corresponding to digital value 511 (see text for explanation).

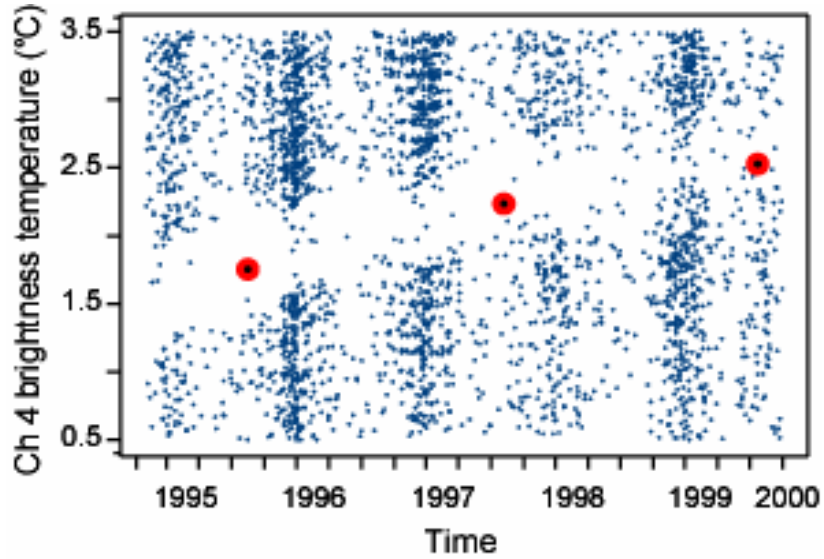


**Figure 3.** SST residuals (in situ minus satellite SST) as a function of in situ SST value, NOAA-14 matchups 1995-1999. Red circles correspond to matchups below the gap (i.e.,  $T_4 \leq 1.5^\circ\text{C}$ ). Blue crosses correspond to matchups with  $3.0^\circ\text{C} \leq T_4 \leq 5.0^\circ\text{C}$ ; these points represent conditions immediately above the gap.

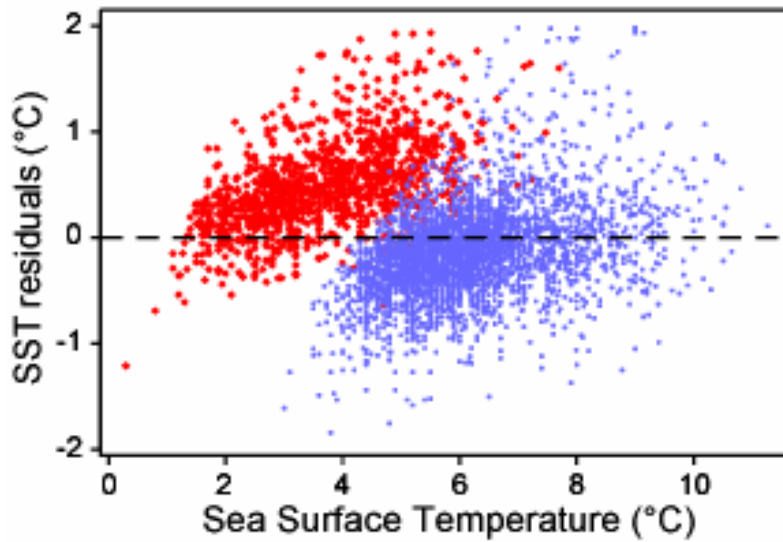


**Figure 4.** Simulated conversion of analog to 4-bit digital values. If the conversion works correctly, all bars should have the same height (not shown). If the threshold for the highest-order bit is modified, this results in a deficit of observations for digital value 8 and a corresponding enhancement (indicated in darker color) of the number of observations for digital value 7.

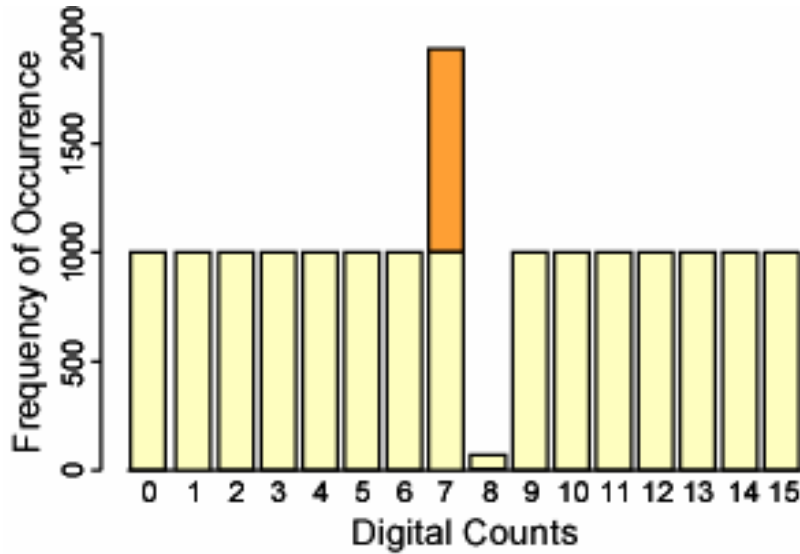


**Figure 5.** Frequency distributions of digital count values for NOAA-14 AVHRR channels 4 (red line) and 5 (blue line), and NOAA-16's channel 4 (green line). The values correspond to data south of 40°S for the period 31 October 2000 to 2 November 2000.

